Conformational Behavior of Cinchonidine Revisited: A Combined Theoretical and Experimental Study

Atsushi Urakawa, Daniel M. Meier, Heinz Rüegger, and Alfons Baiker*

Institute for Chemical and Bioengineering, Department of Chemistry and Applied Biosciences, ETH Zurich, Hönggerberg, HCI, 8093 Zurich, Switzerland

Received: April 13, 2008; Revised Manuscript Received: May 26, 2008

Conformational space of cinchonidine has been explored by means of ab initio potential and free energy surfaces, and the temperature-induced changes of conformational populations were studied by a combined NOESY-DFT analysis. The DFT-derived potential energy surface investigation identified four new conformers. Among them, Closed(7) is substantially relevant to fully understand the conformational behavior. The energy surfaces gave access to the favored transformation pathways at different temperatures (280−320 K). They also revealed the reasons for the negligible presence of energetically stable conformers and explained the experimentally observed temperature dependence of the populations.

Introduction

Cinchona alkaloids have been well-known over the past centuries for their therapeutic efficacy, especially against malaria.[1] Nowadays, the unique combination of the stereogenic centers is beneficially exploited to obtain optically pure compounds by chiral separation,[2,3] homogeneous (organo[4] and organometallic[5]) and heterogeneous catalysis.[6] Figure 1 shows the structure of cinchonidine (CD), one of the most intensively studied cinchona alkaloids concerning the conformational behavior,[7–14] inspired by the seminal extensive work by Dijkstra and co-workers.[15,16] The conformers, characterized by the quinoline and the quinuclidine moieties connected via the chiral alcoholic carbon, can generally be described by two torsional angles, τ_1 and τ_2 (Figure 1) and, in some cases, additionally by the orientation of the hydroxyl group.[9] The conformational behavior of CD is rather complex; it is remarkably influenced by various parameters, such as solvents,[7] solutes,[10,17,18] self-interactions,[14,19] protonation,[12] and the presence of metallic surfaces.[11,20,21] Knowledge on the conformation is critical, because the conformation in solution and on surface can directly influence its chiral interactions with substrates, hence the resulting chemistry. NMR, nuclear Overhauser enhancement spectroscopy (NOESY), IR, vibrational circular dichroism, and theoretical modeling have been applied to study the dynamic aspects of its structure. Still, the determination of the populations of different CD conformers, for example, by NOESY, is a difficult task considering the seven conformers proposed previously.[8,13] Three conformers, Closed(1), Closed(2), and Open(3), have been reported to be substantially populated in solvents of different polarity.[7] In the Closed conformers, the quinuclidine N is oriented toward the quinoline moiety, whereas in the Open conformers, the N points away from the quinoline moiety. The conformational population changes were investigated on the basis of the $^1H-^1H$ vicinal proton coupling constant $^3J_{H8-H9}$ (τ_3, Figure 1).[7] Open(3) has been reported to be the most stable conformer in apolar solvents, whereas the fraction of the Closed conformers drastically rises upon increase of solvent polarity.

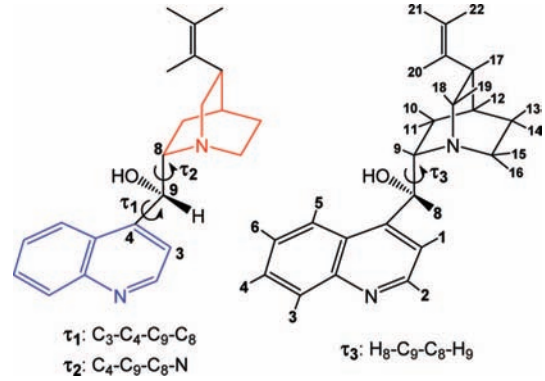

Figure 1. CD atom numbering for the carbon (left) and hydrogen (right) atoms and definition of τ_1, τ_2, and τ_3. The quinoline and quinuclidine moieties of CD are highlighted in blue and red, respectively.

Here, we have revisited the conformational behavior of CD, giving also attention to the influence of temperature, which, to our knowledge, has not been considered in previous studies. Possible conformers of CD are reevaluated on the basis of DFT-derived potential energy surface (PES), and full conformer population analysis is attempted by a combined NOESY-DFT analysis. The influence of the temperature on the conformational behavior and the favored transformation pathways are investigated by using DFT derived free energy surfaces (FESs) obtained by ab initio metadynamics.[22,23]

Methods

NMR. NMR spectra were recorded on a Bruker Avance AV-700 MHz spectrometer. CD (>98%, Fluka) and toluene-d_8 (>99.8%, Dr. Glaser AG Basel) were used as received. A diluted solution of CD (2.5 mM, in toluene) was used to minimize intermolecular interactions and avoid autoaggregation, which deemed necessary in order to compare with theoretical calculations assuming CD in vacuum. Signal assignments were assisted by correlation spectroscopy (COSY) and total correlation spectroscopy (TOCSY). NOESY spectra were obtained with a mixing time of 600 ms. The COSY and TOCSY spectra can be found elsewhere.[24]

* Corresponding author. Tel: +41 44 632 3153. Fax: +41 44 632 1163. E-mail: baiker@chem.ethz.ch.

10.1021/jp803185j CCC: $40.75
Published on Web 07/17/2008

Computational Methods. Two different DFT methods were used in this work: (1) the BLYP functional[25,26] with plane-wave basis sets using CPMD (CPMD, Copyright IBM Corp. 1990–2008, Copyright MPI für Festkörperforschung Stuttgart 1997–2001) and (2) the B3PW91 functional[25,27] with the Gaussian 6-311G(d,p) basis sets using Gaussian 03.[28] These methods are noted hereafter as BLYP-PW and B3PW91-G, respectively. The BLYP-PW method applied plane-wave basis sets with an energy cutoff of 70 Ry within a cubic cell of 24 Å in length. Norm-conserving Troullier−Martins pseudopotentials were used to describe the interaction between the valence electrons and ionic cores.[29] The Hartree potential was computed by the Martina-Tuckerman scheme to mimic the conditions of an isolated system in gas phase.[30] No solvent effects were considered in both methods.

The PES as the function of the two characteristic torsion angles, τ_1 and τ_2, was constructed by a series of geometry optimizations by using the BLYP-PW method where τ_1 and τ_2 were constrained; in other words, all the other geometrical degrees of freedom besides the τ_1 and τ_2 were relaxed and subjected to optimization. The τ_1 and τ_2 were varied from 0 to 360° by an increment of 10° (total $36 \times 36 = 1296$ geometry optimizations). The FES at 200 and 300 K was obtained by ab initio metadynamics[22,23] by using the Car−Parrinello scheme[31] as implemented in CPMD,[23] which had been successfully applied to study free energy profiles in molecular rearrangement,[23,32] phase transitions,[33] and catalysis.[34,35] The two torsion angles τ_1 and τ_2 were taken as the collective variables. The potential hills exerting as the penalty potential were added every 120−300 molecular dynamics steps. The hill height was between 0.03−0.3 kcal/mol. The wave functions were occasionally quenched to the Born−Oppenheimer surface to have the electronic kinetic energy under control. The velocity of the center of mass was set to zero every 1000 molecular dynamics steps to prevent a translational motion. An electronic fictitious mass of 500 au and a time step of 5 au (0.121 fs) were used. The temperature was controlled by rescaling the atomic velocities. The total simulation time was about 330 ps for both temperatures. All the molecular graphics were generated by VMD.[36] The potential and FESs shown are scaled by taking the most stable point as zero energy.

Results and Discussion

CD Conformers—Revisited. Up to now, seven conformers of CD have been described in the literature, namely, Closed(1), Closed(2), Open(3), Open(4), Open(5), and Open(6),[8] as well as the recently reported Open(5)′ where the hydroxyl group forms an internal hydrogen bond with the quinuclidine N.[13] The PES shown in Figure 2, obtained by the BLYP-PW method with a reasonably fine grid size, uncovers several new aspects of the conformation. First, four additional conformers could be identified, namely, Closed(7), Open(8), Open(9), and Open(11). They were named as Closed or Open defined as previously;[8] however, the numbering is arbitrary and does not correspond to the significance of a conformer. In this study, we designate Open(5)′ as Open(10) because of the presence of two other conformers with internal hydrogen bonding, Open(9) and Open(11). The structures of all conformers and their characteristic dihedral angles (τ_1, τ_2, and τ_3) obtained by the BLYP-PW and the B3PW91-G methods are given in Figure 3 and Table 1, respectively. The newly uncovered conformers including Open(10) can be categorized into two groups: those with τ_1 values close to 15°, Closed(7), Open(8), and Open(9), and those with τ_2 values close to 270° (Table 1), Open(9), Open(10), and Open(11). The conformers in the former group have stretched structures, and those in the latter group form internal hydrogen bonds as shown in Figure 3. It is important to note that the actual location of the minima of Open(10) and Open(11) in Figure 2 is likely biased because of the artifacts of the constraint geometry optimizations, which potentially influenced the rotational relaxation of the hydroxyl group. Further refining of minimum energy structure starting from the two minima in Figure 2 reached minima between Open(5) and Open(3) for Open(10) ($\tau_1 = 101.8°$, $\tau_2 = 267.7°$, obtained by the BLYP-PW method) and between Open(6) and Open(4) for Open(11) ($\tau_1 = 279.2°$, $\tau_2 = 272.5°$, by the same method). Vibrational analysis of the conformers (Figure 2 and Table 1) confirmed the stationary nature of the energetic minima by the absence of imaginary frequencies.

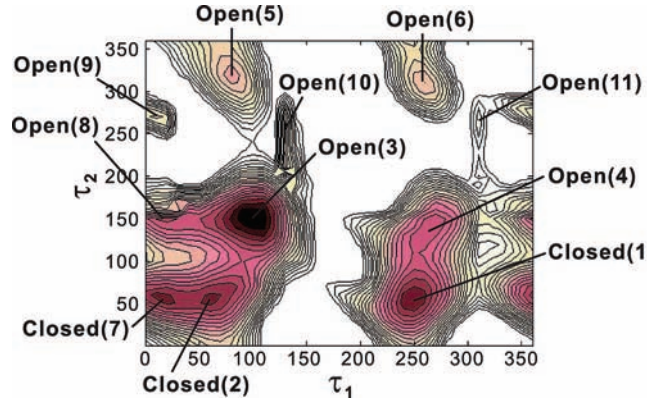

Figure 2. CD conformers mapped on PES. The contour increment of the PES is 0.5 kcal/mol, and the PES was truncated at 10.0 kcal/mol for clarity.

The minimum, previously assigned to Closed(2) and reported to be shallow and broad,[8] in fact consists of two minima, namely, Closed(2) and Closed(7), the latter being energetically more stable (Table 1). Similarly, the reported large minimum of the most stable Open(3) conformer actually contains the minimum of Open(8), the stability of which is similar to that of Open(4). Moreover, both DFT methods confirmed the presence of the remarkably stable conformer with the internal hydrogen bond, Open(10). The structures and relative energies obtained by the BLYP-PW and the B3PW91-G methods were similar. The differences in the dihedral angles were within 10°, except for the τ_1 angles for Closed(2) and Closed(7) where the values are off by 24.7 and 11.2°, respectively. The order of the stability for the first five stable conformers obtained by the B3PW91-G method is as follows: Open(3) > Open(10) > Closed(1) > Closed(7) > Closed(2), whereas the order of Open(10) and Closed(1) is reversed in the BLYP-PW method (Table 1). The presence of Open(10) and Closed(7) within the five most stable conformers and the stability order clearly represent the significance of a more precise exploration of the PES at the DFT level, because they could not be identified previously by molecular mechanics[8,15,37] and semiempirical methods.[9,13] They also imply that the previous consideration of only three stable conformers, Closed(1), Closed(2), and Open(3), as practically relevant ones, is not sufficient to fully understand the conformational behavior of CD.

Temperature-Dependent Population of CD Conformers. The conformation and population changes induced by solvents have been thoroughly investigated and clearly explained.[7] The populations were estimated by the vicinal $^1H-^1H$ coupling constant between H_8-H_9, $^3J_{H8-H9}$, by considering only the three conformers Closed(1), Closed(2), and Open(3) and by assuming the two conformers of the closed type to have the same

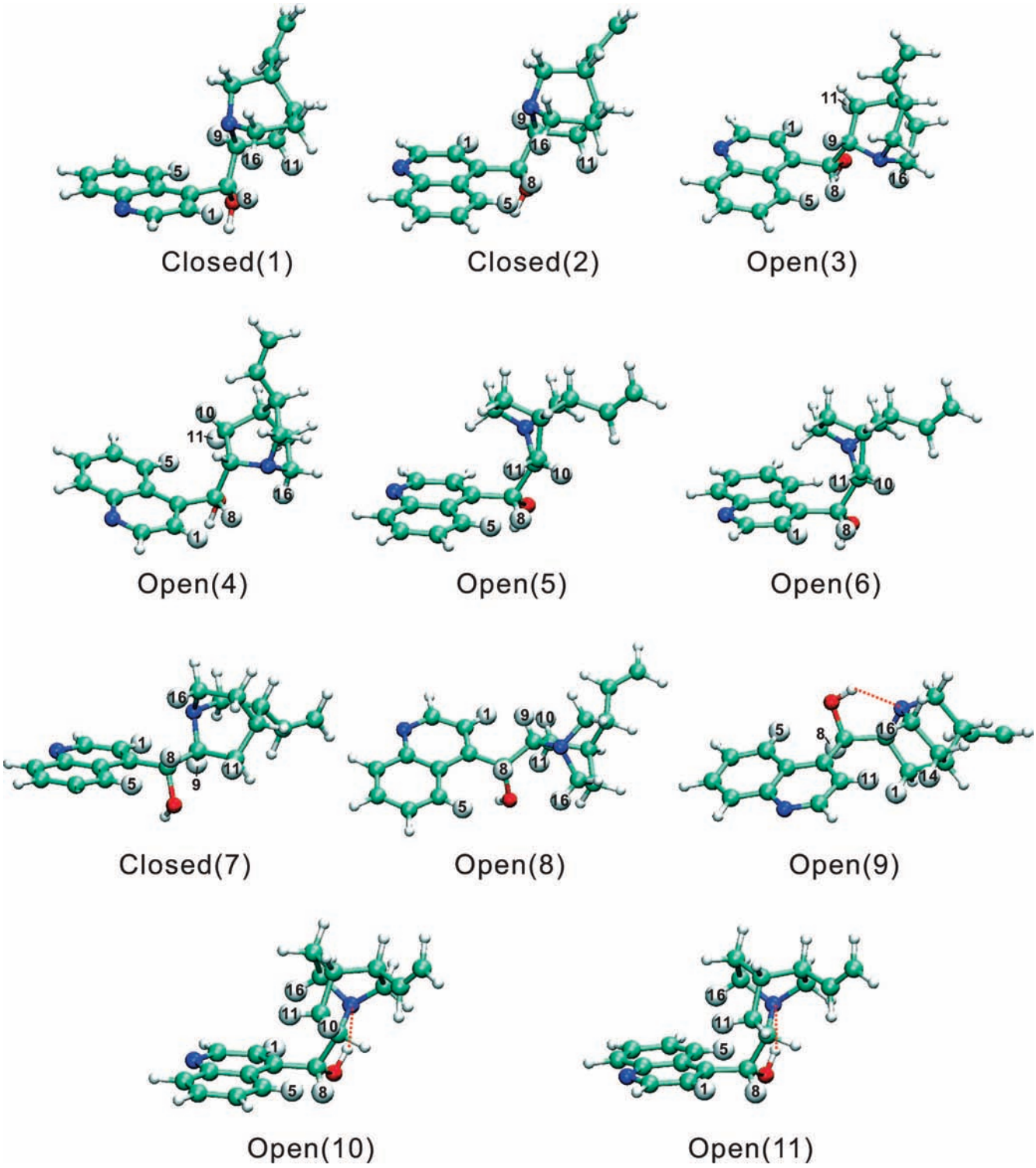

Figure 3. Minimum energy conformations of CD optimized by the BLYP-PW method. Hydrogen atoms which are characteristic for conformer discrimination and having interatomic distances among themselves of less than 3.0 Å are shown by a ball of a larger radius with the numbering according to that in Figure 1.

population.[7] The presence of the four additional conformers shown in the previous section may greatly influence the conclusions drawn in the past. Here, we investigate the conformational population from a combination of NOESY cross-peak volumes and the structural information obtained by the DFT calculations.

The combined analysis, denoted here as NOESY-DFT analysis, simply takes the H−H bond lengths of the different conformers from the DFT calculations and relates them to the cross-peak volumes of specific proton pairs in the 11 conformers. An experimental cross-peak volume V_{i-j} was assumed to be the sum of volume fractions due to a proton pair H_i and H_j with the interatomic distance r_{i-j}, of different conformers k, the population p_k of which is distinct but dependent, satisfying the condition, $\Sigma p_k = 1$. The assumption of a single and constant rotational correlation time τ_e results in a constant product $V_{i-j}(r_{i-j})^6$ ($\equiv C$) for any arbitrary proton pair. Over all conformers, this yields $V_{i-j} = C\Sigma[p_k(r_{i-j})^{-6}]$. By considering

TABLE 1: Characteristic Dihedral Angles (τ_1, τ_2, and τ_3, in Degrees) and Relative Energies (RE, in kcal/mol) of the Investigated CD Conformers

	BLYP-PW				B3PW91-G			
	τ_1	τ_2	τ_3	RE	τ_1	τ_2	τ_3	RE
Closed(1)	248.9	50.1	175.0	1.11	256.2	63.4	190.7	1.58
Closed(2)	60.1	59.9	180.1	1.45	84.8	69.9	193.6	2.08
Open(3)	98.7	150.1	278.2	0.00	102.4	151.6	280.3	0.00
Open(4)	260.2	139.7	271.8	2.57	270.8	148.1	280.8	2.80
Open(5)	88.4	310.5	76.0	5.02	83.5	317.0	82.2	4.98
Open(6)	260.1	309.8	78.5	4.90	261.1	307.2	76.8	4.51
Closed(7)	17.3	52.8	172.7	1.29	6.1	56.5	177.9	1.78
Open(8)	20.0	149.8	277.9	2.29	12.6	152.3	281.2	2.61
Open(9)	10.1	270.0	41.9	6.07	2.5	273.2	45.9	6.97
Open(10)	101.8	267.7	37.7	1.31	102.1	273.4	43.7	1.09
Open(11)	279.2	272.5	46.4	3.87	279.2	271.8	46.4	3.29

only the proton pairs which are less distant than 3 Å and characteristic for the conformer discrimination as shown in Figure 3 (the details can be found in the Supporting Information), the relations for V_{i-j} and Σp_k finally give 15 linear equations for 12 unknowns (all the equations used in this work are described in the Supporting Information). The solution for this obviously inconsistent linear system was approximated simply by the least-squares solution through an orthogonal projection. In reality, the deviations of the actual structures from the DFT-optimized ones due to the methodology itself and solvent effects and also the experimental uncertainties of the NOESY cross-peak volumes lead to considerable errors in the obtained conformational populations. This was particularly noticeable when taking the populations of all 11 conformers as variables, yielding some negative populations. Fortunately, on the basis of the proton-pair distances obtained by the DFT and the cross-peak volumes as well as the relative energies of the conformers, we could omit the contribution of several conformers. Those considered to be relevant in practice were Closed(1), Closed(2), Open(3), Closed(7), and Open(10). Therefore, in addition to the above 15 equations, we added six additional constraining conditions where the populations p_k of the nonrelevant conformers were set to zero.

Figure 4 shows the conformational population of CD at 280, 300, and 320 K obtained by the NOESY-DFT analysis. The B3PW91-G optimized, generally more reliable, structures were used in the analysis. We observed a decrease in Open(3) and an increase in the Closed conformers at higher temperatures. The population change was significant within only 40 K difference; the population of the total Open conformers decreased from 0.83, to 0.75, and to 0.70, at 280, 300, and 320 K, respectively, whereas the total population of the Closed conformers nearly doubled. The population of Closed(7) was consistently higher than that of Closed(2), which confirms the considerable importance of the conformer. The highest stability of Closed(1) among the Closed conformers agrees well with the highest stability found by the DFT methods. The population of Open(10) seems very minor and even in the error range, although it is the most stable conformer after Open(3) by the B3PW91-G method. The PES (Figure 2) suggests that the minimum of Open(10) is distantly located from other low energy minima and/or the energetic barrier to the conformer is high, hindering the visit of the Open(10) minimum. The minor population of Open(10) can be further emphasized in a polar medium due to the intermolecular interaction weakening the internal hydrogen bond and destabilizing the conformer. Moreover, $^3J_{H8-H9}$ analysis gave 3.5, 4.2, and 4.9 Hz at 280, 300, and 320 K, respectively. The calculated $^3J_{H8-H9}$ values based on the populations obtained by the NOESY-DFT analysis at

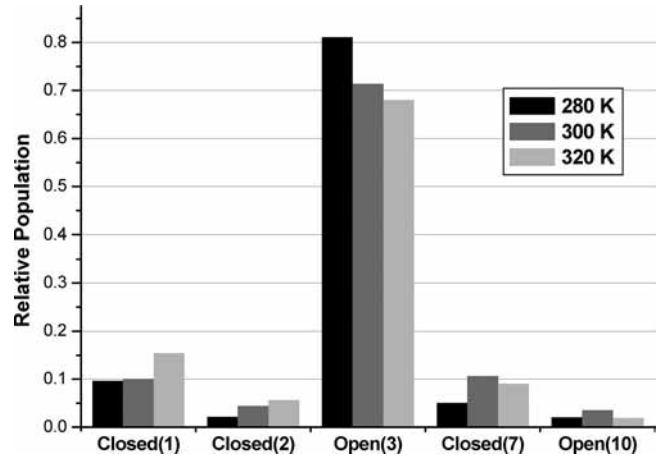

Figure 4. Conformational population of CD at 280, 300, and 320 K obtained by the combined NOESY-DFT analysis.

the respective temperatures (Figure 4) and the modified Karplus[38] equation by Colucci[39] are 2.8, 3.5, and 3.9 Hz. The trend and extent of the increase in the coupling constant were well reproduced; however, the absolute values were ca. 0.8 Hz off. This can be due to errors of the estimated populations and also the idealized substituents taken into account in the calculation. The error of the NOESY-DFT analysis was ca. 10%, estimated from the total errors of the 14 equations for V_{i-j} (see the Supporting Information), which is in an acceptable range considering the rather crude approximations we have taken and the uncertainty of the experimental V_{i-j} values.

CD Conformation from Energy Surface Viewpoints. We further investigate the conformational behavior of CD based on ab initio energy surfaces. In addition to the relative stabilities of the conformers, the transition pathways are accessible from the surfaces. FESs obtained by the ab initio metadynamics at 200 and 300 K in vacuo are shown in Figure 5. For the sake of clear comparison, the PES shown previously (Figure 2) is also presented on the same energy scale. They obviously indicate which pathways are preferred for the conformational changes and the probability of finding the respective conformers. The FESs reproduced the minima of all the conformers identified on the PES, except the apparent minima of Open(10) and Open(11) on the PES. It should be reminded that the actual locations of these minima on the PES were slightly shifted. Actually, the minima of the Open conformers with the internal hydrogen bond are clearly visible on the FES at 300 K (at $\tau_1 \approx 100°$, $\tau_2 \approx 260°$ and at $\tau_1 \approx 275°$, $\tau_2 \approx 275°$), whereas those of Open(5) and Open(6) appear vanished. Careful comparisons of the energy surfaces from 0 K (PES) to 300 K show that, in fact, the minima of Open(5) and Open(6) disappear and shift down in τ_2, finally leading to Open(10) and Open(11). The FES at 300 K shows a much more free rotation along τ_2, clearly seen from the wider channel along τ_2 at about -30 (330) to 160° in τ_1. This enhanced rotation at higher temperature may change the relative population of these conformers, stabilizing Open(10) and destabilizing Open(5). Along this potential and free energy channel, several important insights of the conformational behaviors could be gained. First, the minima of Open(3), Open(8), Closed(2), and Closed(7) merge and form a deep, wide energy well at higher temperature. The preferred transformation pathway between Open(3) and Closed(2)/Closed(7) is greatly influenced by the temperature; at lower temperature, a direct transformation between Open(3) and Closed(2) is preferred, whereas at higher temperature, a deep channel between 40−80° in τ_1 and 80−120° in τ_2 is formed,

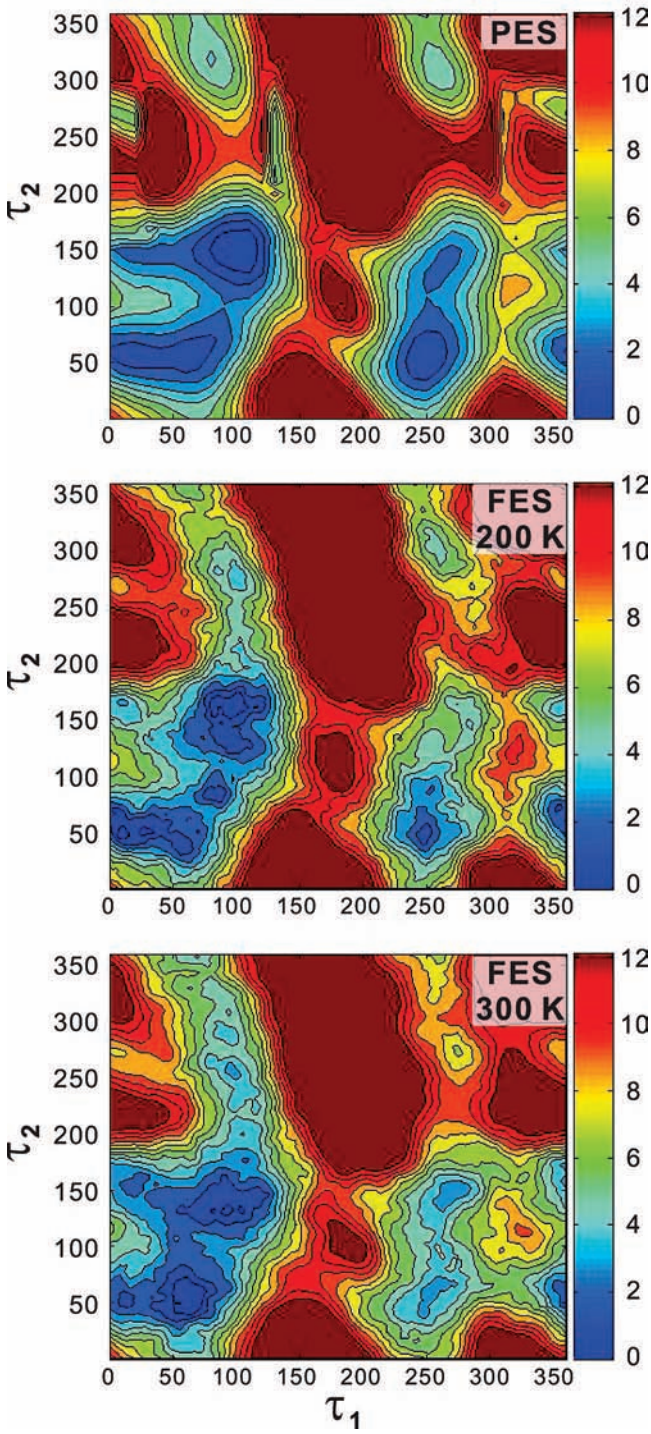

Figure 5. Potential and FES of CD. τ_1 and τ_2 angles are in degrees, and the energy scales shown on the right are shown in kcal/mol. The contour increment of the PES is 1.0 kcal/mol, and the PES was truncated at 13.0 kcal/mol for clarity.

facilitating facile conformational interchanges between the four conformers. Furthermore, the conformational changes via τ_1 rotation through the channels around 320° in τ_1 is evidently favored compared to the route around 160° as clearly visible from the wider and deeper channels connecting the minima. The energetic barrier was estimated by NMR to be ca. 8−11 kcal/mol for CD and dihydroquinidine.[7,40] On the basis of the energy surfaces, we estimate ca. 6−8 kcal/mol for the energy barrier. The underestimation may originate from the absence of solvent in our theoretical models.

The rotation along τ_2 is remarkably hindered in the other channel where τ_1 is between 170 and 320°. The minima of Closed(1) and Open(4) are separated from those of Open(6) and Open(11) by a high energy barrier around 200−230° in τ_2, whereas the transformation probability is higher via the rotation direction where τ_2 decreases (e.g., from Closed(1) to Open(11)). The relative stability of Open(4) is enhanced at 300 K compared to that at 200 K, likely because of the wider channel formed between Open(4) and Open(8) at 300 K, the stability of the latter being also enhanced by the merger of the minimum with Open(3). The populations of Open(4) and Closed(1) seem equivalent from the FES at 300 K, contrary to the absence of Open(4) in our experiments. However, the results of the simulation in vacuo need to be carefully compared to solvated systems because of drastic or specific restriction of the vibrational motions and hence the flexibility of CD. The experimentally obtained conformational information should be compared to that obtained by simulation in vacuo at lower temperatures because of the restricted motion; hence, our experimental conditions could be more comparable to the CD in vacuo at 200 K. On the FES at 200 K, the minimum of Closed(1) is significantly more pronounced than that of Open(4), which is in good agreement with our experimental observation.

The contradiction between the negligible experimental population of Open(10) and its high energetic stability found by the DFT methods can be explained by the energy surface analysis. The energetic minimum of the most stable conformer, Open(3), can be characterized as a wide and deep well. The wide character implies the high entropic stability, accommodating conformational fluctuations. It is even more pronounced at higher temperature, being wider and starting to merge with other energy wells located nearby in the conformational space. Clearly, at 300 K, the minimum of Open(3) merges with Closed(2), Closed(7), and Open(8), enhancing the population of these conformers. This explains the population change, that is, the increase for Closed(2) and Closed(7) and the decrease for Open(3). On the other hand, the narrow and isolated character of Open(10) minimum is likely the reason for the instability of the conformation. In particular, the narrow character signifies the short-range of flexibility and hence the entropic instability of the conformer. At temperature higher than 300 K in vacuo, however, Open(10) minimum may merge with Open(3) minimum, and the population may be enhanced.

In summary, the PES and FESs yielded the energetic barriers and preferred pathways of the overall conformational interchanges, which were not accessible previously. The energy surface exploration at the DFT level revealed four new conformers, and the results are well comparable to our experimental observations obtained by the NOESY-DFT analysis. They evidently explained the population decrease of Open(3) and the gradual increase of all the Closed conformers. Open(3) is likely most populated at any temperature in vacuo and also in apolar medium because of the prominently wide and deep energetic well in the absence of significant interactions with solvent molecules. All energetic wells become wider at higher temperature because of the enhanced flexibility caused by the higher kinetic energy. Especially the very wide and deep well of Open(3) merges to nearby conformers, Closed(2), Closed(7), and Open(8), as well as the conformer with the internal hydrogen bond, Open(10). The second most stable conformer, Closed(1), and the nearby conformer, Open(4), are separated from the other stable conformers by considerable energy barriers. They can form a common wide minimum, but this probably requires significantly higher temperature. The presence of Open(5),

Open(6), and Open(11) are negligible under conditions without any intermolecular interactions, for example, due to polar solvents. The overall picture of PES and FESs clearly shows that temperature greatly influences the conformational behavior of CD and the populations. Very important aspects influencing the conformation such as intermolecular interactions and the effect of solvents and solutes were neglected in this study. Without doubts, a similar analysis considering these effects would lead to a full comprehension of the conformational behavior and will be a future challenge. Although the effect of molecular interactions on the conformation of CD depends specifically on the presence of functional groups of the interacting molecule, the conformational behavior of CD in nonpolar solvents such as toluene, which is frequently applied in asymmetric hydrogenation on cinchona-modified noble metals,[6] is excellently described by the present study. Also, the presence of the conformers with an internal hydrogen bond implies the substantial importance of the direction of the hydroxyl group. Additional dimension in the conformational analysis, such as the dihedral angle of $H-O-C_9-C_8$,[9] may improve the missing influence of the OH direction. Finally, our findings provide insight into another important parameter crucial for stereocontrol, that is, temperature, which affects the conformational behavior of cinchona alkaloids and in turn their role in enantiodifferentiating processes relevant in chiral catalysis and separation.

Conclusions

Conformational space of CD was reevaluated by DFT-based PES. The analysis clarified the energetic minima of four additional conformers. The PES investigation suggested that Closed(7) and Open(10) are as stable as the practically relevant conformers reported previously. Furthermore, the temperature-dependent populations of all the CD conformers were analyzed in detail by combined NOESY-DFT analysis, indicating that the presence of Closed(7) is substantial, whereas that of Open(10) is negligible. The careful analysis of the energy surfaces gave access, in particular, to the entropic stability of each conformer, which explained the experimental conformational population changes. The rather confined energy well is likely responsible for the instability of Open(10). Although this study neglects the influence of solvent and additional solutes, it clearly points out the importance of temperature in the conformational behavior of cinchona alkaloids.

Supporting Information Available: Equations used in the NOESY-DFT analysis, list of proton pairs, their distances, and NOESY cross-peak volumes used in the analysis. This material is available free of charge via the Internet at http://pubs.acs.org.

References and Notes

(1) Saxton, J. E. *Monoterpenoid Indole Alkaloids*; JOHN WILEY & SONS, 1994; Vol. Supplement to Volume 25, Part 4.

(2) Maier, N. M.; Schefzick, S.; Lombardo, G. M.; Feliz, M.; Rissanen, K.; Lindner, W.; Lipkowitz, K. B. *J. Am. Chem. Soc.* **2002**, *124*, 8611.

(3) Wirz, R.; Bürgi, T.; Lindner, W.; Baiker, A. *Anal. Chem.* **2004**, *76*, 5319.

(4) Johansson, C. C. C.; Bremeyer, N.; Ley, S. V.; Owen, D. R.; Smith, S. C.; Gaunt, M. J. *Angew. Chem., Int. Ed.* **2006**, *45*, 6024.

(5) Balavoine, G. G. A.; Manoury, E. *Appl. Organomet. Chem.* **1995**, *9*, 199.

(6) Mallat, T.; Orglmeister, E.; Baiker, A. *Chem. Rev.* **2007**, *107*, 4863.

(7) Bürgi, T.; Baiker, A. *J. Am. Chem. Soc.* **1998**, *120*, 12920.

(8) Schürch, M.; Schwalm, O.; Mallat, T.; Weber, J.; Baiker, A. *J. Catal.* **1997**, *169*, 275.

(9) Caner, H.; Biedermann, P. U.; Agranat, I. *Chirality* **2003**, *15*, 637.

(10) Bürgi, T.; Vargas, A.; Baiker, A. *J. Chem. Soc., Perkin Trans. 2* **2002**, 1596.

(11) Calvo, S. R.; LeBlanc, R. J.; Williams, C. T.; Balbuena, P. B. *Surf. Sci.* **2004**, *563*, 57.

(12) Olsen, R. A.; Borchardt, D.; Mink, L.; Agarwal, A.; Mueller, L. J.; Zaera, F. *J. Am. Chem. Soc.* **2006**, *128*, 15594.

(13) Vargas, A.; Bonalumi, N.; Ferri, D.; Baiker, A. *J. Phys. Chem. A* **2006**, *110*, 1118.

(14) Margitfalvi, J. L.; Talas, E.; Zsila, F.; Kristyan, S. *Tetrahedron: Asymmetry* **2007**, *18*, 750.

(15) Dijkstra, G. D. H.; Kellogg, R. M.; Wynberg, H.; Svendsen, J. S.; Marko, I.; Sharpless, K. B. *J. Am. Chem. Soc.* **1989**, *111*, 8069.

(16) Dijkstra, G. D. H.; Kellogg, R. M.; Wynberg, H. *J. Org. Chem.* **1990**, *55*, 6121.

(17) Ferri, D.; Bürgi, T.; Baiker, A. *J. Chem. Soc., Perkin Trans. 2* **2002**, 437.

(18) Ferri, D.; Bürgi, T.; Baiker, A. *J. Chem. Soc., Perkin Trans. 2* **1999**, 1305.

(19) Williams, T.; Pitcher, R. G.; Bommer, P.; Gutzwill, J.; Uskokovi, M. *J. Am. Chem. Soc.* **1969**, *91*, 1871.

(20) Ferri, D.; Bürgi, T. *J. Am. Chem. Soc.* **2001**, *123*, 12074.

(21) Vargas, A.; Baiker, A. *J. Catal.* **2006**, *239*, 220.

(22) Laio, A.; Parrinello, M. *Proc. Natl. Acad. Sci. U.S.A.* **2002**, *99*, 12562.

(23) Iannuzzi, M.; Laio, A.; Parrinello, M. *Phys. Rev. Lett.* **2003**, *90*, 238302.

(24) Meier, D. M.; Urakawa, A.; Rüegger, H.; Baiker, A. *J. Phys. Chem. A* **2008**, DOI: 10.1021/jp801866p.

(25) Becke, A. D. *Phys. Rev. A* **1988**, *38*, 3098.

(26) Lee, C. T.; Yang, W. T.; Parr, R. G. *Phys. Rev. B* **1988**, *37*, 785.

(27) Perdew, J. P.; Wang, Y. *Phys. Rev. B* **1992**, *45*, 13244.

(28) Frisch, M. J.; Trucks, G. W.; Schlegel, H. B.; Scuseria, G. E.; Robb, M. A.; Cheeseman, J. R.; Montgomery, J. A., Jr.; Vreven, T.; Kudin, K. N.; Burant, J. C.; Millam, J. M.; Iyengar, S. S.; Tomasi, J.; Barone, V.; Mennucci, B.; Cossi, M.; Scalmani, G.; Rega, N.; Petersson, G. A.; Nakatsuji, H.; Hada, M.; Ehara, M.; Toyota, K.; Fukuda, R.; Hasegawa, J.; Ishida, M.; Nakajima, T.; Honda, Y.; Kitao, O.; Nakai, H.; Klene, M.; Li, X.; Knox, J. E.; Hratchian, H. P.; Cross, J. B.; Bakken, V.; Adamo, C.; Jaramillo, J.; Gomperts, R.; Stratmann, R. E.; Yazyev, O.; Austin, A. J.; Cammi, R.; Pomelli, C.; Ochterski, J. W.; Ayala, P. Y.; Morokuma, K.; Voth, G. A.; Salvador, P.; Dannenberg, J. J.; Zakrzewski, V. G.; Dapprich, S.; Daniels, A. D.; Strain, M. C.; Farkas, O.; Malick, D. K.; Rabuck, A. D.; Raghavachari, K.; Foresman, J. B.; Ortiz, J. V.; Cui, Q.; Baboul, A. G.; Clifford, S.; Cioslowski, J.; Stefanov, B. B.; Liu, G.; Liashenko, A.; Piskorz, P.; Komaromi, I.; Martin, R. L.; Fox, D. J.; Keith, T.; Al-Laham, M. A.; Peng, C. Y.; Nanayakkara, A.; Challacombe, M.; Gill, P. M. W.; Johnson, B.; Chen, W.; Wong, M. W.; Gonzalez, C.; Pople, J. A. *Gaussian 03*, revision C.02; Gaussian, Inc.: Wallingford, CT, 2004.

(29) Troullier, N.; Martins, J. L. *Phys. Rev. B* **1991**, *43*, 1993.

(30) Hockney, R. W. *The potential calculation and some applications*; Academic Press: New York/London, 1970; Vol. 9.

(31) Car, R.; Parrinello, M. *Phys. Rev. Lett.* **1985**, *55*, 2471.

(32) Stirling, A.; Iannuzzi, M.; Laio, A.; Parrinello, M. *ChemPhysChem* **2004**, *5*, 1558.

(33) Oganov, A. R.; Martonak, R.; Laio, A.; Raiteri, P.; Parrinello, M. *Nature* **2005**, *438*, 1142.

(34) Stirling, A.; Iannuzzi, M.; Parrinello, M.; Molnar, F.; Bernhart, V.; Luinstra, G. A. *Organometallics* **2005**, *24*, 2533.

(35) Urakawa, A.; Iannuzzi, M.; Hutter, J.; Baiker, A. *Chem.—Eur. J.* **2007**, *13*, 6828.

(36) Humphrey, W.; Dalke, A.; Schulten, K. *J. Mol. Graphics* **1996**, *14*, 33.

(37) Carroll, F. I.; Abraham, P.; Gaetano, K.; Mascarella, S. W.; Wohl, R. A.; Lind, J.; Petzoldt, K. *J. Chem. Soc., Perkin Trans. 1* **1991**, 3017.

(38) Karplus, M. *J. Chem. Phys.* **1959**, *30*, 11.

(39) Colucci, W. J.; Jungk, S. J.; Gandour, R. D. *Magn. Reson. Chem.* **1985**, *23*, 335.

(40) Aune, M.; Gogoll, A.; Matsson, O. *J. Org. Chem.* **1995**, *60*, 1356.

JP803185J